Mineralogical Magazine, June 2014, Vol. 78(3), pp. 583–590

Tondiite, $Cu_3Mg(OH)_6Cl_2$, the Mg-analogue of herbertsmithite

T. Malcherek[1,*], L. Bindi[2], M. Dini[3], M. R. Ghiara[4,5], A. Molina Donoso[6], F. Nestola[7], M. Rossi[4,5] and J. Schlüter[1]

[1] Mineralogisch-Petrographisches Institut, Universität Hamburg, Grindelallee 48, D-20146 Hamburg, Germany
[2] Dipartimento di Scienze della Terra, Università di Firenze, via La Pira, 4, I-50121, Florence, Italy
[3] Pasaje San Augustin, 4045 La Serena, Chile
[4] Centro Musei delle Scienze Naturali e Fisiche, Real Museo Mineralogico, Università di Napoli Frederico II, Via Mezzocannone, 8, I-80138 Naples, Italy
[5] Dipartimento di Scienze della Terra, dell'Ambiente e delle Risorse, Università di Napoli Federico II, Largo san Marcellino 10. 80138 Naples, Italy
[6] Los Algarrobos, 2986 Iquique, Chile
[7] Dipartimento di Geoscienze, Università di Padova, Via G. Gradenigo, 6, I-35131 Padua, Italy

[*Received 22 December 2014; Accepted 6 February 2014; Associate Editor: S.J. Mills*]

ABSTRACT

Tondiite, with the simplified formula $Cu_3Mg(OH)_6Cl_2$, occurs as a rare supergene mineral in a phonolitic tephrite from the type locality, Vesuvius volcano, Italy, as well as associated with haydeeite in the Santo Domingo Mine, Arica Province, Chile. It is emerald green to bright green in colour and occurs in irregularly shaped crystals, often with stepped faces. Its calculated density is 3.503 g cm^{-3}. Tondiite crystallizes with the herbertsmithite structure type, space group $R\bar{3}m$. Lattice parameters are a = 6.8377(7) Å and c = 14.088(2)Å for the holotype material. The c parameter may vary with Mg/Cu ratio and the presence of impurity atoms. The five strongest lines in the calculated powder diffraction pattern are [d in Å(I)($hkil$)]: 5.459(88)(10$\bar{1}$1), 3.419(22)(11$\bar{2}$0), 2.764(100)(11$\bar{2}$3), 2.266(54)(02$\bar{2}$4), 1.706(26)(22$\bar{4}$0). Several tondiite crystals have been examined by single-crystal X-ray diffraction and by electron microprobe analysis. The observed Mg content ranges between 0.6 and 0.7 atoms per formula unit. The structural role of Mg is discussed.

Keywords: herbertsmithite, new mineral, basic copper chloride, Vesuvius, Caleta Vitor, haydeeite.

Introduction

Among the secondary Cu minerals, atacamite, $Cu_2(OH)_3Cl$, hosts divalent Cu exclusively in heterogenous six-fold coordination, either coordinated by five OH groups and one Cl anion or by four OH groups and two apical Cl anions. The atacamite structure is not expected to tolerate significant concentrations of metal cations other than Cu^{2+} (Braithwaite *et al.*, 2004). However, different structural configurations of the basic Cu chlorides can enhance the tolerance for such substitutions. Formal exchange of Cl and OH anions across adjacent $Cu(OH)_5Cl$ polyhedra of atacamite (Malcherek and Schlüter, 2010) converts half of the $Cu(OH)_5Cl$ polyhedra into $Cu(OH)_6$-coordination environments, while the other half becomes $Cu(OH)_4Cl_2$. As a result of the Jahn-Teller effect, the $Cu(OH)_6$ octahedra are strongly elongated, but substitution of Cu^{2+} by other cations such as Zn^{2+} or Mg^{2+} results in more regular six-fold coordination. These substitutions give rise to a series of trigonal or pseudo-trigonal polymorphs which, in the example of Zn substitution, extend from pure $Cu_2(OH)_3Cl$, i.e. clinoatacamite (Grice *et al.*, 1996) or anatacamite

* E-mail: thomas.malcherek@uni-hamburg.de
DOI: 10.1180/minmag.2014.078.3.08

(Malcherek and Schlüter, 2009) *via* paratacamite $Cu_3(Cu,Zn)(OH)_6Cl_2$ (Fleet, 1975; Braithwaite *et al.*, 2004), towards herbertsmithite, $Cu_3Zn(OH)_6Cl_2$ (Braithwaite *et al.*, 2004). Gillardite, $Cu_3Ni(OH)_6Cl_2$ (Clissold *et al.*, 2007) and leverettite, $Cu_3Co(OH)_6Cl_2$ (Kampf *et al.*, 2013*b*) are isostructural with herbertsmithite. Like herbertsmithite they crystallize in space group $R\bar{3}m$ and constitute the corresponding endmembers for Ni and Co substitution of pseudo-trigonal $Cu_2(OH)_3Cl$.

The present report is concerned with the Mg-analogue of herbertsmithite, with idealized composition $Cu_3Mg(OH)_6Cl_2$. The mineral and the name tondiite have been approved by the International Mineralogical Association Commission on New Minerals, Nomenclature and Classification (IMA2013-077). Tondiite is named in honour of Matteo Tondi (1762–1835), eminent Italian mineralogist and collaborator of René J. Haüy in writing the classic *Traitè de Mineralogie.* Holotype material is deposited in the mineralogical collections of the Real Museo Mineralogico di Napoli, Università di Napoli, Italy, catalogue number 1178R.

Tondiite is already known as a synthetic compound (Colman *et al.*, 2011). The minerals of the entire atacamite group and herbertsmithite in particular, have received much attention for their magnetic properties in recent years. This is due to geometrical frustration of antiferromagnetic ordering within the so-called kagome layers of Cu atoms, which are ideally magnetically insulated in herbertsmithite. The herbertsmithite structure is often described in terms of intralayer sites (ideally occupied by Cu) and interlayer sites (ideally occupied by Zn). Magnesium constitutes the interlayer cation in tondiite (Fig. 1).

While the mineral haydeeite (Schlüter and Malcherek, 2007) has a similar chemical composition to tondiite, it exhibits a different crystal structure (Malcherek and Schlüter, 2007), composed of layers that contain the Cu atoms in a kagome arrangement and the Mg atoms in the

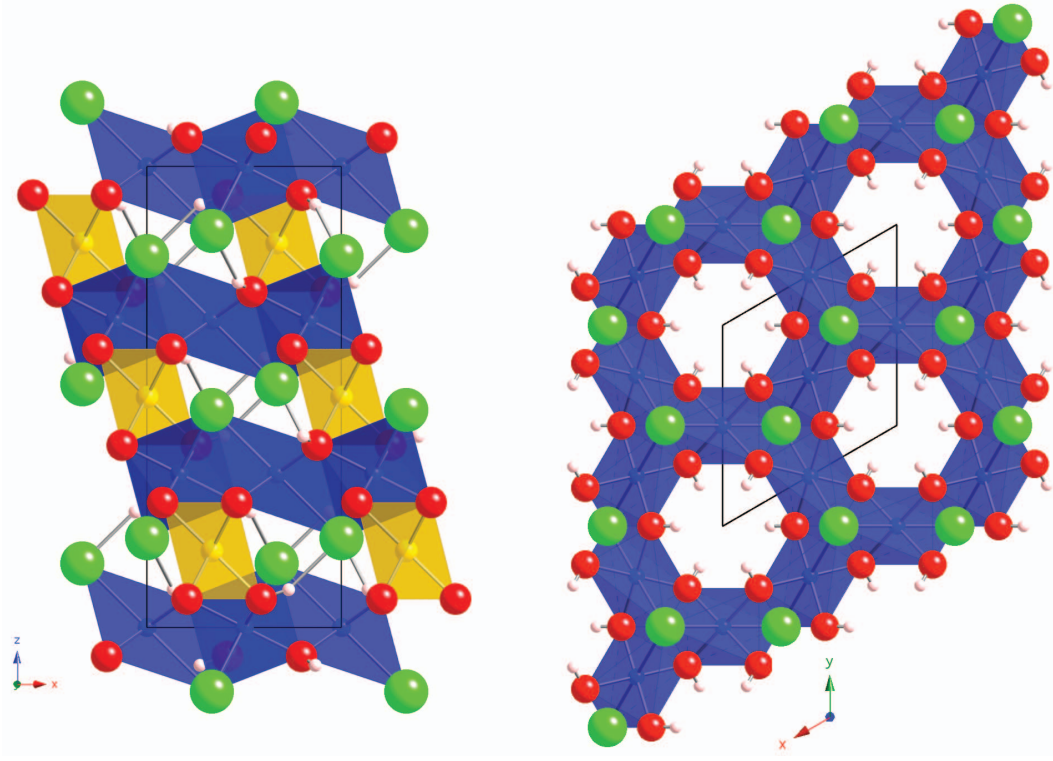

FIG. 1. The crystal structure of tondiite, viewed along $\mathbf{a}_2$ and along **c**, showing the stacking of the Cu kagome layers with Mg atoms occupying the interlayer space (left) and an individual kagome layer (right). Colour scheme, in order of sphere size: H = pink, Cu = blue, Mg = yellow, O = red, Cl = green.

interstices of this two-dimensional lattice. The layers connect vertically only *via* H bonding. Haydeeite crystallizes in space group $P\bar{3}m1$ and is isostructural with kapellasite, $Cu_3Zn(OH)_6Cl_2$ (Krause *et al.*, 2006). Paratacamite-(Mg), $Cu_3(Cu,Mg)(OH)_6Cl_2$, has recently been described by Kampf *et al.* (2013*a*), as the Mg-analogue of paratacamite. The paratacamite structure is characterized by a doubled *a*-lattice repeat with respect to herbertsmithite and can be identified by the appearance of weak superstructure reflections, while a hexagonal metric is maintained. Paratacamite transforms reversibly to herbertsmithite at elevated temperatures (Welch *et al.*, 2014).

Results and discussion

Occurence

The holotype specimen of tondiite (sample I) was not found *in situ* but came from an old sample belonging to the Collezione Vesuviana of the Real Museo Mineralogico, Universitá di Napoli, Italy. The rock specimen was labelled as '1906 lava' with catalog number 1178R and was contained in a wooden box labelled as '1906 erupted lavas'. The observed mineral assemblage supports the data that the rock is a phonolitic-tephrite-vesicular lava erupted from the Vesuvius volcano in 1906. Tondiite was found in mm-sized vesicles in the volcanic rock by oine of the authors (MR). Associated minerals are leucite, sodalite, nepheline, sanidine and Fe oxides and hydroxides. Tondiite was also found by one of the authors (AMD) in the Santo Domingo Cu mine (18º45′51″S, 70º18′16″W), Caleta Vitor district, Arica province, Chile, where tondiite occurs as a supergene alteration product together with haydeeite, anhydrite and atacamite. The primary mineralization occurs in veins embedded in andesitic porphyric lavas and lava tuff flows, banded by calcareous limestone. The mine has been exploited in the past for its high Cu sulfide content (Mortimer *et al.*, 1971) and has not yet been abandoned. Tondiite appears to be an oxidation product of chalcocite, bornite and chalcopyrite in an environment rich in Cl, typical of the Atacama desert. Crystals from this location are denoted as sample II below. This cotype material is preserved in the collection of the Mineralogical Museum, University of Hamburg, Germany with catalogue number MD480.

Optical and physical properties

Tondiite is optically uniaxial (+), ω = 1.749(6) and ε = 1.766(7) (589 nm). It occurs as emerald green to bright green transparent crystals with vitreous lustre (Fig. 2). Mohs hardness is 3–3.5. Its calculated density from holotype empirical formula and unit-cell parameters is 3.503 g cm^{-3}. Crystals of tondiite show slight pleochroism in transmitted light, changing from green to faintly green. Dominant forms are {101} and {012}. Crystals of sample II show characteristic steps along their most pronounced faces.

Chemical composition

The chemical composition of both mineral samples was determined using wavelength-dispersive electron microprobe analysis (Table 1). As the

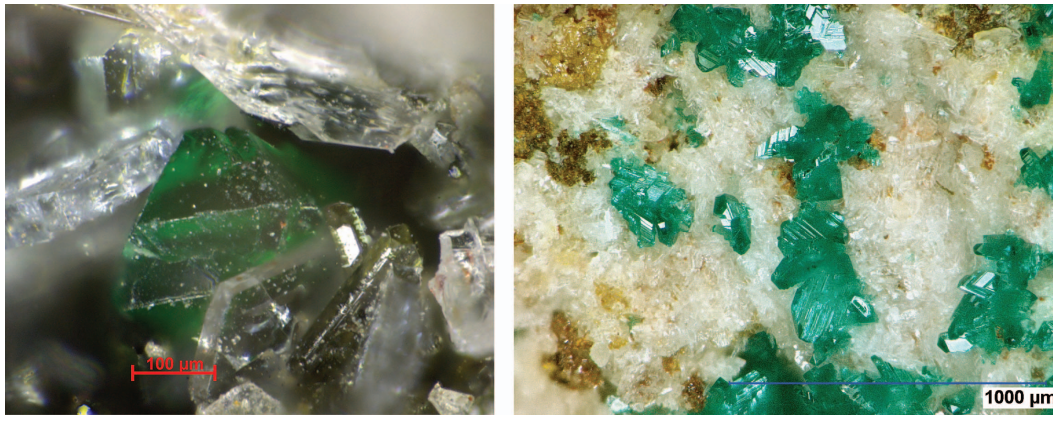

FIG. 2. Emerald green crystal of the holotype tondiite from Italy (sample I, left). Tondiite from Chile (sample II, right).

amount of material available is insufficient for direct analysis of H_2O, H_2O has been calculated based on the assumption that, apart from Cl^-, $(OH)^-$ is the only anionic species in tondiite. Zinc was below the detection limit in both samples. Fifteen spots were analysed on sample I (20 kV, 20 nA and 10 μm beam diameter), 20 spots on sample IIb (15 kV, 20 nA and focused beam).

The empirical formula of tondiite based on 8 anions per formula unit (p.f.u.) is $Cu_{3.29}Mg_{0.65}Mn_{0.05}(OH)_{6.11}Cl_{1.89}$ according to analysis of the holotype sample I and $Cu_{3.38}Mg_{0.62}(OH)_{6.06}Cl_{1.94}$ for sample IIb from Chile. The simplified formula is $Cu_3Mg(OH)_6Cl_2$ which requires (wt.%) 61.52 CuO, 10.39 MgO, 13.94 H_2O and 18.28 Cl (−4.12 O = Cl).

X-ray diffraction

Single crystal X-ray diffraction was carried out using Mo*K*α radiation on a STOE Stadi IV diffractometer equipped with an Agilent CCD area detector (sample I) and on a Nonius KappaCCD diffractometer (sample II). Data from two crystals have been collected in the case of sample II (IIa and IIb) and processed using the *Eval15* suite of programs (Schreurs *et al.*, 2010). Absorption effects were corrected using *Sadabs*. The structure was refined using *JANA2006* (Petříček *et al.*, 2006). Crystal IIb was later used for microprobe analysis.

Structure refinement of tondiite confirms the herbertsmithite structure. No deviation of lattice parameters from hexagonal metrics was detected. No evidence for additional reflections, indicative of the paratacamite cell with $a' = 2a$ has been obtained. Crystal IIb exhibits weak additional reflections caused by twinning. The twin domain can be obtained by −112.2º rotation about the normal to $(\bar{1}11)$.

The composition obtained from structure refinement is $Cu_{3.35}Mg_{0.65}(OH)_6Cl_2$ (sample I) and $Cu_{3.296}Mg_{0.704}(OH)_6Cl_2$ (sample IIa) and $Cu_{3.396}Mg_{0.603}(OH)_6Cl_2$ (sample IIb). These compositions agree well with the respective results from electron microprobe analysis obtained for sample I and IIb. While the *a* lattice parameter shows little variation across all compositions reported in Table 2, the *c* lattice parameter varies between 14.088 and 14.002 Å. The particularly large value of *c* for the holotype material might be due to the sample's Mn content.

Structural parameters obtained for crystal IIa are shown in Tables 3 and 4. The atomic positions

TABLE 1. Results of electron microprobe analysis of samples I and II. H_2O has been calculated based on equimolarity of O and H.

Sample	I (Italy)				IIb (Chile)			
	wt.%	Range	esd	Standard	wt.%	Range	esd	Standard
CuO	65.90	62.74–67.98	1.50	Cu	66.78	65.11–68.57	0.85	CuO
MnO	0.94	0.58–1.92	0.37	Rhodonite	n.d.			
MgO	6.61	5.34–9.20	1.14	Periclase	6.12	4.54–6.79	0.65	MgO
Cl	16.79	15.88–17.63	0.70	KCl	17.05	16.76–17.34	0.14	Vanadinite
H_2O	13.84				13.52			
O=Cl	−3.79				−3.85			
Total	100.29				99.62			

n.d.: not detected.

refined for the other two crystals agree with these values within two estimated standard deviations (esd). Selected interatomic distances and angles are given in Table 5. A distance restraint of 1.00±0.03 Å was applied to the primary O–H bond. Calculated X-ray powder diffraction data for tondiite are given in Table 6.

The structure model used for refining sample I and sample IIa and IIb locates Mg entirely on the interlayer, 3*b* Wyckoff site. This contrasts with the structure refinements reported for synthetic crystals (Chu *et al.*, 2010) and powders (Colman *et al.*, 2011; Kermarrec *et al.*, 2011), where small but significant concentrations of Mg on the intralayer 9*e* site were detected by site-occupancy refinement against Cu. This scenario was checked for sample IIa, where shared occupancy of the 9*e* site by Cu and Mg seems to suggest a Mg occupancy of ~4%, albeit with no further improvement of the residual. As the Mg occupancy at the 3*b* site is hardly affected by the additional parameter, the total refined Mg content rises to 0.86 atoms p.f.u., in contradiction to the chemical analysis.

To further investigate the possible substitution of Mg for Cu at the intralayer sites, it is worthwhile considering the central assumptions involved in the structure model that are invoked here. One of these assumptions is that the electron density of the atoms is spherical about their

TABLE 2. Details of crystals and structure refinements for samples I and II in comparison with literature data of synthetic samples.

	Sample studied, this work			Chu *et al.* (2011)	Colman *et al.* (2011)
	I	IIa	IIb		
X_{Mg}	0.163	0.176*	0.155	0.1875	0.2405
X_{Mg}(Cu2)	0.65(3)*	0.704(4)*	0.603(4)*	0.607(8)*	0.827(9)
a (Å)	6.8377(7)	6.8345(2)	6.8384(2)	6.8322(11)	6.83886(1)
c (Å)	14.088(2)	14.0022(7)	14.0103(5)	13.960(2)	14.02125(3)
V (Å^3)	570.4(1)	566.42(4)	567.40(3)	564.33(15)	567.917(2)
Space group	$R\bar{3}m$				
λ (Å)	0.7107				0.41226
T (K)	295	295(1)	295(1)	100(2)	295
ρ_{calc} (g cm^{-3})	3.503	3.514	3.541	3.512	3.416
Absorption coef., μ (mm^{-1})	10.887	9.936	10.18	9.851	n.a.
T_{min}	0.732	0.627	0.563	0.285	n.a.
T_{max}	0.814	0.747	0.747	0.320	n.a.
R_{int}	0.094	0.026	0.021	0.034	n.a.
θ_{max}	43.19	35	35	30	17.5
Observed refl.	$F > 4\sigma(F)$	$I > 3\sigma(I)$		$I > 2\sigma(I)$	n.a.
$N_{meas.}$	9876	8914	7612	2792	n.a.
N_{all}	491	340	353	228	n.a.
N_{obs}	442	339	352	219	n.a.
R_{obs}	0.064	0.0128	0.0144	0.0162	n.a.
GooF	1.14	1.04	1.22	1.194	n.a.
N_{par}	18	21	22	21	n.a.
Weighting	$1/(\sigma^2(F_o^2)+(wP)^2+kP)$ $P = (F_o^2+2F_c^2)/3$ w = 0.0401 k = 30.0496	$1/(\sigma^2(I)+wI^2)$ w = 0.0025		$1/(\sigma^2(F_o^2)+(wP)^2+kP)$ $P = (F_o^2+2F_c^2)/3$ w = 0.0202 k = 1.5278	n.a.
Extinction coef.	0.006(1)	0.0033(3)	0.170(17)	0.0090(7)	n.a.
$\Delta\rho_{max}$ (e Å^{-3})	2.90	0.16	0.15	n.a.	n.a.
$\Delta\rho_{min}$ (e Å^{-3})	−2.02	−0.12	−0.13	n.a.	n.a.

* Value from X-ray structure refinement.
N_{meas}: number of reflections measured; N_{all}: number of unique reflections; N_{obs}: number of observed reflectons; N_{par}: number of parameters
n.a.: not available

TABLE 3. Atomic parameters of tondiite (sample IIa). The equivalent isotropic displacement parameter, U_{eqv}, in Å^2.

Site	*x*	*y*	*z*	U_{eqv}	Occupancy
Cu1	0.5	0	0	0.0102(1)	
Cu2	0	0	0.5	0.0088(2)	0.704(4)Mg / 0.296(4)Cu
Cl	0	0	0.19432(3)	0.0139(2)	
O	0.20646(7)	$-x$	0.06214(6)	0.0125(2)	
H	0.136(2)	$-x$	0.082(2)	0.031(7)	

TABLE 4. Refined anisotropic displacement parameters in Å^2 (sample IIa).

Site	U^{11}	U^{22}	U^{33}	U^{12}	U^{13}	U^{23}
Cu1	0.0097(1)	0.0090(2)	0.0118(2)	$U^{22}/2$	0.00093(2)	$2U^{13}$
Cu2	0.0102(2)	U^{11}	0.0060(3)	$U^{11}/2$	0	0
Cl	0.0154(2)	U^{11}	0.0111(2)	$U^{11}/2$	0	0
O	0.0108(2)	U^{11}	0.0162(4)	0.0056(2)	0.0019(1)	$-U^{13}$

centre. In order to reduce the possible effects of discrepancies between this model and the real electron density in tondiite, reflections at small scattering angles ($\sin\theta/\lambda < 0.5$, equivalent to 26% of observed reflections) were temporarily removed from the data set. While this has a relatively small effect on the Mg occupancy at the 3*b* site (0.68), it drastically reduces the refined Mg content at the 9*e* site to trace levels. This indicates that the small amount of Mg refined at the intralayer sites of tondiite is an artefact of the structure model, rather than a realistic estimate of Mg atoms occupying these sites. Significant Mg occupancy on intralayer *Cu* sites might still occur for total Mg concentrations in excess of 0.7 atoms p.f.u., but it can be disregarded for our mineral samples.

Raman spectroscopy

The Raman spectrum of tondiite (I) between 300 and 1200 cm^{-1} was collected using a confocal Raman microscope (Jasco, NRS-3100). The 647 nm line of a water-cooled Kr^+ laser (Innova 300, Coherent), was channeled into an integrated Olympus microscope and focused to a spot size of ~3 μm by a 20× objective with a final power of 6 mW at the sample. A holographic notch filter was used to reject the excitation laser line. The Raman backscatter data were collected at 180º, using a 0.1 mm slit and a diffraction lattice of 1200 groove/mm, corresponding to an average resolution of 4 cm^{-1}. It takes five accumulations (60 s each) to collect a complete data set by a Peltier-cooled 1024 × 128 pixel CCD photon detector (Andor DU401BVI). Wavelength

TABLE 5. Selected interatomic distances (Å) and angles (º) for sample IIa.

Cu1–O (×4)	1.9856(5)	O–Cu1–O	81.85(3)
Cu1–Cl (×2)	2.7716(4)	O–Cu1–Cl	82.51(2)
Cu2–O (×6)	2.0971(7)	O–Cu2–O	76.66(3)
O–H	0.88(2)	O–H–Cl	154(2)
Cl–H (×3)	2.25(2)		
Cu1–Cu1	3.4172(3)		
Cu1–Cu2	3.0559(2)		

TABLE 6. Calculated X-ray powder diffraction data for tondiite. Intensity and d_{hkil} were calculated using the software *POWDER CELL 2.3* (Kraus and Nolze, 1996) on the basis of the structural model for sample I. The strongest reflections are given in bold.

h	*k*	*i*	*l*	d_{calc}	$I_{rel.}$
1	**0**	**$\bar{1}$**	**1**	**5.459**	**88**
0	0	0	3	4.696	2
0	1	$\bar{1}$	2	4.533	4
1	**1**	**$\bar{2}$**	**0**	**3.419**	**22**
0	**2**	**$\bar{2}$**	**1**	**2.898**	**15**
1	**1**	**$\bar{2}$**	**3**	**2.764**	**100**
2	0	$\bar{2}$	2	2.729	12
0	0	0	6	2.348	12
0	**2**	**$\bar{2}$**	**4**	**2.266**	**54**
2	1	$\bar{3}$	1	2.210	4
2	0	$\bar{2}$	5	2.041	8
3	0	$\bar{3}$	0	1.974	2
1	1	$\bar{2}$	6	1.936	3
1	0	$\bar{1}$	7	1.906	12
2	1	$\bar{3}$	4	1.889	1
3	0	$\bar{3}$	3	1.820	8
0	**3**	**$\bar{3}$**	**3**	**1.820**	**19**
1	2	$\bar{3}$	5	1.752	2
2	**2**	**$\bar{4}$**	**0**	**1.709**	**26**
0	2	$\bar{2}$	7	1.664	1
1	3	$\bar{4}$	1	1.631	5
3	1	$\bar{4}$	2	1.599	1
2	0	$\bar{2}$	8	1.513	5
3	0	$\bar{3}$	6	1.511	2
2	1	$\bar{3}$	7	1.496	12
4	0	$\bar{4}$	1	1.472	2
0	4	$\bar{4}$	2	1.448	3
1	1	$\bar{2}$	9	1.423	3
1	2	$\bar{3}$	8	1.384	2
2	**2**	**$\bar{4}$**	**6**	**1.382**	**13**
1	0	$\bar{1}$	10	1.370	1
4	0	$\bar{4}$	4	1.365	6
3	2	$\bar{5}$	1	1.352	3
0	4	$\bar{4}$	5	1.310	2

calibration was performed using cyclohexane as standard. Raman microscopy measurements on three different spots were performed on the crystals as a test of homogeneity and reproducibility.

Due to the very weak signal, only five well distinguished Raman peaks could be measured which are (in order of decreasing intensity) at 363, 503, 942, 395 and 695cm^{-1} (Fig. 3). As reported for infrared (IR) spectroscopy on herbertsmithite (Braithwaite *et al.*, 2004), the peaks in the

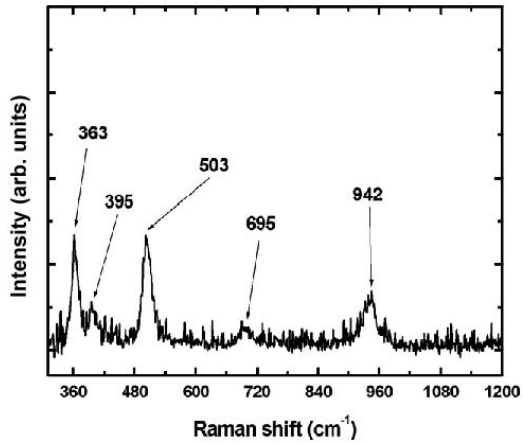

FIG. 3. Raman spectrum of the holotype tondiite from Italy between 300 and 1200 cm^{-1}.

700–1000 cm^{-1} region can be assigned to CuO–H and MgO–H deformations. In detail, the peaks at 942 and 695 cm^{-1} could be assigned to in-plane and out-of-plane CuO–H and MgO–H deformations. Peaks in the region 360–500 cm^{-1} should be due to metal–O stretching vibrations. The position of the band at 942 cm^{-1} is noteworthy. Braithwaite *et al.* (2004) proposed a simple discrimination basis for the minerals belonging to the herbertsmithite–paratacamite–clinoatacamite series based on the position of an IR absorption band in the same frequency range. Those authors showed that the monoclinic minerals of the series have this band between 920 and 930 cm^{-1}, whereas the rhombohedral ones show it at values >935 cm^{-1}. Tondiite exhibits a Raman signal at 942 cm^{-1} in perfect agreement with the crystal symmetry observed by means of X-ray diffraction.

Acknowledgements

Peter Stutz and Stefanie Heidrich in Hamburg are thanked for sample preparation and microprobe analysis, respectively.

References

Braithwaite, R.S.W., Mereiter, K., Paar, W.H. and Clark, A.M. (2004) Herbertsmithite, $Cu_3Zn(OH)_6Cl_2$, a new species, and the definition of paratacamite. *Mineralogical Magazine*, **68**, 527–539.

Chu, S., McQueen, T.M., Chisnell, R., Freedman, D.E., Müller, P., Lee, Y.S. and Nocera, D.G. (2010) A

Cu^{2+} (S = 1/2) kagome antiferromagnet: $Mg_xCu_{4-x}(OH)_6Cl_2$. *Journal of the American Ceramics Society*, **132**, 5570–5571.

Clissold, M.E., Leverett, P., Williams, P.A., Hibbs, D.E. and Nickel, E.H. (2007) The structure of gillardite, the Ni-analogue of herbertsmithite, from Widgiemooltha, Western Australia. *The Canadian Mineralogist*, **45**, 317–320.

Colman, R.H., Sinclair, A. and Wills, A.S. (2011) Magnetic and crystallographic studies of Mg-herbertsmithite, γ-$Cu_3Mg(OH)_6Cl_2$, a new S = 1/2 kagome magnet and candidate spin liquid. *Chemistry of Materials*, **23**, 1811–1817.

Fleet, M.E. (1975) The crystal structure of paratacamite, $Cu_2(OH)_3Cl$. *Acta Crystallographica*, **B31**, 183–187.

Grice, J.D., Szymański, J.T. and Jambor, J.L. (1996) The crystal structure of clinoatacamite, a new polymorph of $Cu_2(OH)_3Cl$. *The Canadian Mineralogist*, **34**, 73–78.

Kampf, A.R., Sciberras, M.J., Leverett, P., Williams, P.A., Malcherek, T., Schlüter, J., Welch, M., Dini, M. and Molina Donoso, A.A. (2013*a*) Paratacamite-(Mg), $Cu_3(Mg,Cu)Cl_2(OH)_6$ a new substituted basic copper chloride mineral from Camerones, Chile. *Mineralogical Magazine*, **77**, 3113–3123.

Kampf, A.R., Sciberras, M.J., Williams, P.A., Dini, M. and Molina Donoso, A.A. (2013*b*) Leverettite from the Torrecillas mine, Iquique province, Chile: the co-analogue of herbertsmithite. *Mineralogical Magazine*, **77**, 3047–3054.

Kermarrec, E., Mendels, P., Bert, F., Colman, R.H., Wills, A.S., Strobel, P., Bonville, P., Hillier, A. and Amato, A. (2011) Spin-liquid ground state in the frustrated kagome antiferromagnet $MgCu_3(OH)_6Cl_2$. *Physical Review B*, **84**, 100401.

Kraus, W. and Nolze, G. (1996) *POWDER CELL* a program for the representation and manipulation of crystal structures and calculation of the resulting X-ray powder patterns. *Journal of Applied Crystallography*, **29**, 301–303.

Krause, W., Bernhardt, H., Braithwaite, R.S.W., Kolitsch, U. and Pritchard, R. (2006) Kapellasite, $Cu_3Zn(OH)_6Cl_2$, a new mineral from Lavrion, Greece, and its crystal structure. *Mineralogical Magazine*, **70**, 329–340.

Malcherek, T. and Schlüter, J. (2007) $Cu_3MgCl_2(OH)_6$ and the bond valence parameters of the OH–Cl bond. *Acta Crystallographica*, **B63**, 157–160.

Malcherek, T. and Schlüter, J. (2009) Structures of the pseudo-trigonal polymorphs of $Cu_2(OH)_3Cl$. *Acta Crystallographica*, **B65**, 334–341.

Malcherek, T. and Schlüter, J. (2010) Anatacamite from La Vendida mine, Sierra Gorda, Atacama desert, Chile: a triclinic polymorph of $Cu_2(OH)_3Cl$, *Neues Jahrbuch für Mineralogie – Abhandlungen*, **187**, 307–312.

Mortimer, C., Saric, N. and Cáceres, R. (1971) *Apuntes sobre minas de la región costera, provincia de Tarapacá*. Instituto de Investigaciones Geológicas, Iquique, Chile.

Petříček, V., Dušek, M. and Palatinus, L. (2006) *JANA2006. The crystallographic computing system*. Institute of Physics, Prague.

Schlüter, J. and Malcherek, T. (2007) Haydeeite, $Cu_3Mg(OH)_6Cl_2$, a new mineral from the Haydee mine, Salar Grande, Atacama desert, Chile. *Neues Jahrbuch für Mineralogie – Abhandlungen*, **184**, 39–43.

Schreurs, A.M.M., Xian, X. and Kroon-Batenburg, L.M.J. (2010) *EVAL15*: a diffraction data integration method based on *ab initio* predicted profiles. *Journal of Applied Crystallography*, **43**, 70–82.

Welch, M.D., Sciberras, M.J., Williams, P.A., Leverett, P., Schlüter, J. and Malcherek, T. (2014) A temperature-induced reversible transformation between paratacamite and herbertsmithite. *Physics and Chemistry of Minerals*, **41**, 33–48.